SCIENCE CHINA
Information Sciences

• **Supplementary File** •

Adaptive NN impedance control for an SEA-driven robot

Xinbo YU[1, 2, 3], Wei HE[1, 2, 3*], Yanan LI[4], Chengqian XUE[1, 2, 3], Yongkun SUN[1, 2, 3] & Yu WANG[5]

[1]*School of Automation and Electrical Engineering, University of Science and Technology Beijing, Beijing* 100083*, China;*
[2]*Institute of Artificial Intelligence, University of Science and Technology Beijing, Beijing* 100083*, China;*
[3]*Key Laboratory of Knowledge Automation for Industrial Processes, Ministry of Education, University of Science and Technology Beijing, Beijing* 100083*, China;*
[4]*Department of Engineering and Design, University of Sussex, Brighton* BN1 9RH*, UK;*
[5]*Institute of Automation, Chinese Academy of Sciences, Beijing* 100190*, China*

Appendix A Close-loop stability analysis under controller (14):

We construct Lyapunov function candidates as follows

$$V_1 = \frac{1}{2}z^T M_c z + \frac{1}{2}\eta^T M_p \eta + \frac{1}{2}\int_0^t (z-\eta)^T dt K_p \int_0^t (z-\eta)dt. \tag{A1}$$

Differentiating (**??**) with respect to time, we have

$$\begin{aligned}\dot{V}_1 &= z^T M_c \dot{z} + \frac{1}{2}z^T \dot{M}_c z + \eta^T M_p \dot{\eta} + (z-\eta)^T K_p \int_0^t (z-\eta)dt \\ &= z^T (M_c \dot{z} + C_c z + K_p \int_0^t (z-\eta)dt) + \eta^T (M_p \dot{\eta} - K_p \int_0^t (z-\eta)dt).\end{aligned} \tag{A2}$$

We divide (**??**) to two parts, and the first part can be calculated as

$$M_c \dot{z} + C_c z + K_p \int_0^t (z-\eta)dt = M_c(\ddot{q} - \ddot{q}_d + T\dot{e} - \dot{\tau}_{rl}) + C_c(\dot{q} - \dot{q}_d + Te - \tau_{rl}) + K_p(e - \tilde{\vartheta} - e(0) + \tilde{\vartheta}(0) + \beta_\vartheta \int_0^t (e - \tilde{\vartheta})dt)). \tag{A3}$$

According to the robot's dynamic model (1), we obtain

$$M_c \ddot{q} + C_c \dot{q} + G_c - K_p(\vartheta - q) + \tau_f = 0. \tag{A4}$$

Substituting (**??**) to (**??**), we obtain

$$\begin{aligned}M_c \dot{z} + C_c z + K_p \int_0^t (z-\eta)dt = M_c(-\ddot{q}_d + T\dot{e} - \dot{\tau}_{rl}) + C_c(-\dot{q}_d + Te - \tau_{rl}) \\ + K_p(\vartheta_d - q_d - e(0) + \tilde{\vartheta}(0) + \beta_\vartheta \int_0^t (e - \tilde{\vartheta})dt) - G_c - \tau_f.\end{aligned} \tag{A5}$$

Then we rewrite (**??**) as

$$M_c \dot{z} + C_c z + K_p \int_0^t (z-\eta)dt = \zeta_1 + K_p \vartheta_d. \tag{A6}$$

We define $K_p \vartheta_d$ as

$$K_p \vartheta_d = -K_1 z - \zeta_1, \tag{A7}$$

where

$$\zeta_1 = -\tau_f - G_c + M_c(-\ddot{q}_d + T\dot{e} - \dot{\tau}_{rl}) + C_c(-\dot{q}_d + Te - \tau_{rl}) + K_p(-q_d - e(0) + \tilde{\vartheta}(0) + \beta_\vartheta \int_0^t (e - \tilde{\vartheta})dt)). \tag{A8}$$

* Corresponding author (email: weihe@ieee.org)
† The corresponding author is Wei He. The authors declare that they have no conflict of interest.

So ϑ_d can be defined as follows

$$\vartheta_d = K_p^{-1}(-K_1 z + \tau_f + G_c - M_c(-\ddot{q}_d + T\dot{e} - \dot{\tau}_{rl}) - C_c(-\dot{q}_d + Te - \tau_{rl}) - K_p(-q_d - e(0) + \tilde{\vartheta}(0) + \beta_\vartheta \int_0^t (e - \tilde{\vartheta})dt)). \tag{A9}$$

Substituting (**??**) to (**??**), we writte (**??**) as

$$\dot{V}_1 = -z^T K_1 z + \eta^T (M_p \dot{\eta} - K_p \int_0^t (z - \eta)dt) = -z^T K_1 z + \eta^T \zeta_2, \tag{A10}$$

where $\zeta_2 = M_p\dot{\eta} - K_p \int_0^t (z-\eta)dt$, and we rewrite ζ_2 as follows

$$\zeta_2 = M_p \dot{\eta} - K_p \int_0^t (z - \eta)dt = M_p(\ddot{\vartheta} - \ddot{\vartheta}_d + \beta_\vartheta \dot{\tilde{\vartheta}}) - K_p(e - \tilde{\vartheta} - e(0) + \tilde{\vartheta}(0) + \beta_\vartheta \int_0^t (e - \tilde{\vartheta})dt)). \tag{A11}$$

According to SEA's dynamic model (1), we have

$$M_p \ddot{\vartheta} + K_p(\vartheta - q) = \tau. \tag{A12}$$

We define

$$\zeta_2 = \tau + \zeta_3 = -K_2 \eta, \tag{A13}$$

where

$$\zeta_3 = M_p(-\ddot{\vartheta}_d + \beta_\vartheta \dot{\tilde{\vartheta}}) - K_p(-q_d + \vartheta_d - e(0) + \tilde{\vartheta}(0) + \beta_\vartheta \int_0^t (e - \tilde{\vartheta})dt)). \tag{A14}$$

We design the controller τ according to (**??**) and (**??**) as follows

$$\tau = -K_2\eta + M_p(\ddot{\vartheta}_d - \beta_\vartheta \dot{\tilde{\vartheta}}) - z + \tau_f + G_c + M_c(\ddot{q}_d - T\dot{e} + \dot{\tau}_{rl}) + C_c(\dot{q}_d - Te + \tau_{rl}). \tag{A15}$$

We can obtain (**??**) as follows

$$\dot{V}_1 = -z^T K_1 z - \eta^T K_2 \eta \leqslant 0. \tag{A16}$$

Therefore, we can conclude that $t \to 0$, z and η will converge to zero, and error signals e and $\tilde{\vartheta}$ will converge to zero.

Appendix B Close-loop stability analysis under controller (18):

We construct Lyapunov function candidates V_2 as follows

$$V_2 = \frac{1}{2} z^T M_c z + \frac{1}{2}\eta^T M_p \eta + \frac{1}{2}\int_0^t (z-\eta)^T dt K_p \int_0^t (z-\eta)dt + \frac{1}{2}\tilde{\chi}_M^T \Gamma_M^{-1} \tilde{\chi}_M + \frac{1}{2}\tilde{\chi}_C^T \Gamma_C^{-1} \tilde{\chi}_C + \frac{1}{2}\tilde{\chi}_G^T \Gamma_G^{-1} \tilde{\chi}_G. \tag{B1}$$

According to the proof of ***Appendix A***, we can conclude that one part $\dot{V}_{2p}$ of $\dot{V}_2$ can be obtained as

$$\begin{aligned} \dot{V}_{2p} &= -z^T K_1 z + \eta^T(\tau + \zeta_3) \\ &= -z^T K_1 z + \eta^T(\tau + M_p(-\ddot{\vartheta}_d + \beta_\vartheta \dot{\tilde{\vartheta}}) + z - \tau_f - G_c - M_c \dot{A} - C_c A), \end{aligned} \tag{B2}$$

where $A{=}\dot{q}_d - Te + \tau_{rl}$, and by differentiating (**??**) with respect to time, we have

$$\dot{V}_2 = -z^T K_1 z + \eta^T(\tau + M_p(-\ddot{\vartheta}_d + \beta_\vartheta \dot{\tilde{\vartheta}}) + z - \tau_f - G_c - M_c\dot{A} - C_c A) + \Gamma_M^{-1}\tilde{\chi}_M^T \dot{\tilde{\chi}}_M + \Gamma_C^{-1}\tilde{\chi}_C^T \dot{\tilde{\chi}}_C + \Gamma_G^{-1}\tilde{\chi}_G^T \dot{\tilde{\chi}}_G. \tag{B3}$$

Substituting NN controller (18) into (**??**), we have

$$\begin{aligned} \dot{V}_2 = &-z^T K_1 z + \eta^T(-K_2\eta + M_p(\ddot{\vartheta}_d - \beta_\vartheta \dot{\tilde{\vartheta}}) - z + \tau_f + \hat{\chi}_G^T \phi_G(Z) + \hat{\chi}_M^T \phi_M(Z)\dot{A} + \hat{\chi}_C^T \phi_C(Z) A \\ &+ M_p(-\ddot{\vartheta}_d + \beta_\vartheta \dot{\tilde{\vartheta}}) + z - \tau_f - G_c - M_c\dot{A} - C_c A) + \Gamma_M^{-1}\tilde{\chi}_M^T \dot{\tilde{\chi}}_M + \Gamma_C^{-1}\tilde{\chi}_C^T \dot{\tilde{\chi}}_C + \Gamma_G^{-1}\tilde{\chi}_G^T \dot{\tilde{\chi}}_G. \end{aligned} \tag{B4}$$

According to (16), we can rewrite (**??**) as follows

$$\begin{aligned} \dot{V}_2 =& - z^T K_1 z + \eta^T(-K_2\eta + M_p(\ddot{\vartheta}_d - \beta_\vartheta \dot{\tilde{\vartheta}}) - z + \tau_f + \hat{\chi}_G^T \phi_G(Z) + \hat{\chi}_M^T \phi_M(Z)\dot{A} + \hat{\chi}_C^T \phi_C(Z) A \\ &+ M_p(-\ddot{\vartheta}_d + \beta_\vartheta \dot{\tilde{\vartheta}}) + z - \tau_f - G_c - M_c\dot{A} - C_c A) + \Gamma_M^{-1}\tilde{\chi}_M^T \dot{\tilde{\chi}}_M + \Gamma_C^{-1}\tilde{\chi}_C^T \dot{\tilde{\chi}}_C + \Gamma_G^{-1}\tilde{\chi}_G^T \dot{\tilde{\chi}}_G \\ =& - z^T K_1 z + \eta^T(-K_2\eta + \hat{\chi}_G^T \phi_G(Z) + \hat{\chi}_M^T \phi_M(Z)\dot{A} + \hat{\chi}_C^T \phi_C(Z) A - G_c - M_c\dot{A} - C_c A) \\ &+ \Gamma_M^{-1}\tilde{\chi}_M^T \dot{\tilde{\chi}}_M + \Gamma_C^{-1}\tilde{\chi}_C^T \dot{\tilde{\chi}}_C + \Gamma_G^{-1}\tilde{\chi}_G^T \dot{\tilde{\chi}}_G \\ =& - z^T K_1 z + \eta^T(-K_2\eta - K_q \mathrm{sgn}(\eta) + \epsilon_M \dot{A} + \epsilon_C A + \epsilon_G - \chi_M^{*T}\phi_M(Z)\dot{A} - \chi_C^{*T}\phi_C(Z)A - \chi_G^{*T}\phi_G(Z) \\ &+ \hat{\chi}_G^T \phi_G(Z) + \hat{\chi}_M^T \phi_M(Z)\dot{A} + \hat{\chi}_C^T \phi_C(Z)A) + \Gamma_M^{-1}\tilde{\chi}_M^T \dot{\tilde{\chi}}_M + \Gamma_C^{-1}\tilde{\chi}_C^T \dot{\tilde{\chi}}_C + \Gamma_G^{-1}\tilde{\chi}_G^T \dot{\tilde{\chi}}_G \\ =& - z^T K_1 z + \eta^T(-K_2\eta - K_q \mathrm{sgn}(\eta) + B + \tilde{\chi}_M \phi_M(Z)\dot{A} + \tilde{\chi}_C \phi_C(Z) A + \tilde{\chi}_G \phi_G(Z)) \\ &+ \Gamma_M^{-1}\tilde{\chi}_M^T \dot{\tilde{\chi}}_M + \Gamma_C^{-1}\tilde{\chi}_C^T \dot{\tilde{\chi}}_C + \Gamma_G^{-1}\tilde{\chi}_G^T \dot{\tilde{\chi}}_G, \end{aligned} \tag{B5}$$

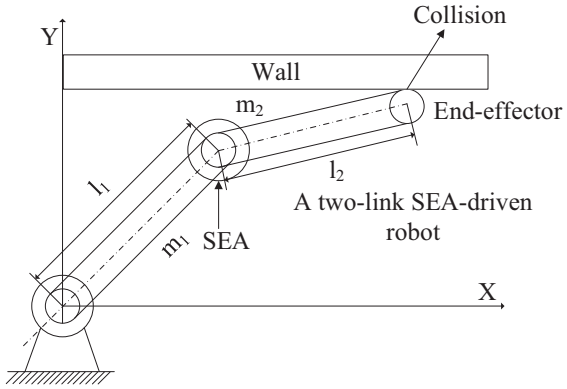

Figure C1 A 2-DOF SEA-driven rotary robot

where $B = \epsilon_M \dot{A} + \epsilon_C A + \epsilon_G$, and $K_q \geqslant ||B||$. Substituting (17) to (**??**), we obtain

$$\begin{aligned}\dot{V}_2 = &-z^T K_1 z - \eta^T K_2 \eta + \eta^T (B - K_q \mathrm{sgn}(\eta)) + \tilde{\chi}_M \phi_M(Z)\dot{A} + \tilde{\chi}_C \phi_C(Z) A + \tilde{\chi}_G \phi_G(Z)) \\ &-\tilde{\chi}_M^T \phi_M(Z)\dot{A}\eta - \tilde{\chi}_C^T \phi_C(Z) A\eta - \tilde{\chi}_G^T \phi_G(Z) - \tilde{\chi}_M^T \sigma_M \hat{\chi}_M - \tilde{\chi}_C^T \sigma_C \hat{\chi}_C - \tilde{\chi}_G^T \sigma_G \hat{\chi}_G. \end{aligned} \tag{B6}$$

Thus, we can obtain that

$$\dot{V}_2 \leqslant -z^T K_1 z - \eta^T K_2 \eta - \frac{\sigma_M}{2}\tilde{\chi}_M^T \tilde{\chi}_M - \frac{\sigma_C}{2}\tilde{\chi}_C^T \tilde{\chi}_C - \frac{\sigma_G}{2}\tilde{\chi}_G^T \tilde{\chi}_G + \frac{1}{2}(\sigma_M \chi_M^{*T} \chi_M^* + \sigma_C \chi_C^{*T} \chi_C^* + \sigma_G \chi_G^{*T} \chi_G^*). \tag{B7}$$

Then we can conlude that variables z and η are bounded and satisfy conditions as follows

$$\begin{aligned}&\lambda_{K_1}||z||^2 + \lambda_{K_2}||\eta||^2 + \frac{\sigma_M}{2}||\mathrm{vec}(\tilde{\chi}_M)||^2 + \frac{\sigma_C}{2}||\mathrm{vec}(\tilde{\chi}_C)||^2 + \frac{\sigma_G}{2}||\mathrm{vec}(\tilde{\chi}_G^T)||^2 \\ &\leqslant \frac{\sigma_M}{2}||\mathrm{vec}(\chi_M^*)||^2 + \frac{\sigma_C}{2}||\mathrm{vec}(\chi_C^*)||^2 + \frac{\sigma_G}{2}||\mathrm{vec}(\chi_G^*)||^2, \end{aligned} \tag{B8}$$

where λ_{K_1} and λ_{K_2} are the minimal eigenvalues of K_1 and K_2, respectively. vec$(\cdot)$ stands for the column vectorization operation. They follow that z and η can be made arbitrarily small by choosing sufficiently large λ_{K_1} and λ_{K_2}. They will converge to zero for σ_M, σ_C and σ_G are all zero. The above inequality can be proved by contradiction: assuming the above inequality is invalid yields $\dot{V}_2 < 0$ and thus V_2 decreases iteratively. This indicates that $||z||$, $||\eta||$, $||\mathrm{vec}(\tilde{\chi}_M)||$, $||\mathrm{vec}(\tilde{\chi}_C)||$ and $||\mathrm{vec}(\tilde{\chi}_G)||$ (and thus the left-hand side of the above inequality) become even smaller, which contradicts the hypothesis.

Appendix C Simulation settings and results

We consider a 2-DOF SEA-driven rotary robot, m_1, m_2 and l_1, l_2 denote the mass and length of links $1, 2$ respectively, where m_1=2.0kg, m_2=0.85kg, l_1=1.40m, l_2=1.24m. The initial position is set as [0.85m; 0.1m], and the desired trajectory is given as $[(0.1\sin(t) + \cos(t))\mathrm{m}; \sin(0.2t)\mathrm{m}]$. When robot's end-effector is tracking the desired trajectory, there is a wall at $y = 0.4$m and robot will collide with the wall shown in Figure **??**. The centers of RBFNNs are chosen in the region of $[-1, 1] \times [-1, 1] \times [-1, 1] \times [-1, 1] \times [-1, 1] \times [-1, 1] \times [-1, 1] \times [-1, 1]$, the NN node is chosen as 2^8, the initial value of the NN weight is set as 0. Γ_M, Γ_C and Γ_G are selected as [100, 0; 0, 100], and σ_M=σ_C=σ_G=0.02. The gain matrices K_1 and K_2 are chosen as $[30, 0; 0, 30]$ and $[40, 0; 0, 40]$. We suppose that the stiffness parameter of the wall is 500 N/m, the SEA inertia matrix M_p is set as [1, 0; 0, 1], the stiffness matrix is set as $[60, 0; 0, 60]$, the desired stiffness in impedance control is set as 20 N/m. We consider two situations that the robot with SEA and without SEA has collisions with the wall. Figure 1 shows the position and the position error of the end-effector in task space, and it also shows that the interaction force with SEA is smaller than the robot without SEA at the beginning of collisions. Therefore, we can conclude that the external force with SEA is smaller than the external force without SEA when physical collisions occur at the first time, and both of them can achieve the desired impedance relationship between force and state error by our proposed adaptive impedance control.

References

1 Lozano R, Brogliato B. Adaptive control of robot manipulators with flexible joints. IEEE T Automat Contr, 1992, 37(2): 174-181
2 Li Y, Ganesh G, Jarrass N, et al. Force, Impedance, and trajectory learning for contact tooling and haptic identification. IEEE T Robot, 2018
3 Li Z, Huang Z, He W, et al. Adaptive impedance control for an upper limb robotic exoskeleton using biological signals. IEEE T Ind Electron, 2017, 64(2): 1664-1674
4 Yang C, Jiang Y, Li Z, et al. Neural control of bimanual robots with guaranteed global stability and motion precision. IEEE T Ind Inform, 2017, 13(3): 1162-1171

5 Ficuciello F, Villani L, Siciliano B. Variable impedance control of redundant manipulators for intuitive human C robot physical interaction. IEEE T Robot, 2015, 31(4): 850-863

6 Calinon S, Guenter F, Billard A. On learning, representing, and generalizing a task in a humanoid robot. IEEE T Syst Man Cy B, 2007, 37(2): 286-298

7 Zhang S, Dong Y, Ouyang Y, et al. Adaptive neural control for robotic manipulators with output constraints and uncertainties. IEEE T Neur Net Lear, 2018

8 Wang D, He H, Liu D. Adaptive critic nonlinear robust control: A survey. IEEE T Cybernetics, 2017, 47(10): 3429-3451

9 Liu Y-J, Tong S, Chen C P, et al. Neural controller design-based adaptive control for nonlinear MIMO systems with unknown hysteresis inputs. IEEE T Cybernetics, 2016, 46(1): 9-19

10 Wang F-Y, Zheng N-N, Cao D P, et al. Parallel driving in CPSS: a unified approach for transport automation and vehicle intelligence. IEEE/CAA Journal of Automatica Sinica, 2017, 4(4): 577-587

11 Xu B, Shi Z, Sun F, et al. Barrier Lyapunov function based learning control of hypersonic flight vehicle with AOA constraint and actuator faults. IEEE T Cybernetics, 2018

12 He W, Meng T, He X, et al. Unified Iterative Learning Control for Flexible Structures with Input Constraints. Automatica, 2018, 86: 326-336

13 Chen M, Ren Y, Liu, J. Antidisturbance control for a suspension cable system of helicopter subject to input nonlinearities, IEEE T Syst Man Cy A, 2017

14 Rozo L, Calinon S, Caldwell D G, et al. Learning physical collaborative robot behaviors from human demonstrations. IEEE T Robot, 2016, 32(3): 513-527

15 Dai S-L, Wang M, Wang C. Neural learning control of marine surface vessels with guaranteed transient tracking performance. IEEE T Ind Electron, 2016, 63(3): 1717-1727

16 Li Y, Tee K P, Chan W L, et al. Continuous role adaptation for human C robot shared control. IEEE T Robot, 2015, 31(3): 672-681

17 Yang C, Zeng C, Liang P, et al. Interface design of a physical human-robot interaction system for human impedance adaptive skill transfer. IEEE T Autom Sci Eng, 2018, 15(1): 329-340

18 Chen M, Ge S S. Adaptive neural output feedback control of uncertain nonlinear systems with unknown hysteresis using disturbance observer. IEEE T Ind Electron, 2015, 62(12): 7706-7716

19 Wang H, Wang C, Chen W, et al. Three-dimensional dynamics for cable-driven soft manipulator. IEEE-ASME T Mech, 2017, 22(1): 18-28

20 Zhang W, Sun F, Wu H, et al. A framework for the fusion of visual and tactile modalities for improving robot perception. SCI CHINA Inf Sci, 2017, 60(1): 012201

21 Huang P, Wang D, Meng Z, et al. Impact dynamic modeling and adaptive target capturing control for tethered space robots with uncertainties. IEEE-ASME T Mech, 2016, 21(5): 2260-2271